

Published in final edited form as:

*Eur J Med Genet.* 2012 February ; 55(2): 128–131. doi:10.1016/j.ejmg.2011.12.005.

## A balanced t(10;15) translocation in a male patient with developmental language disorder

A. Gulhan Ercan-Sencicek, Ph.D.<sup>1</sup>, Nicole R. Davis Wright<sup>1</sup>, Stephan J. Sanders<sup>1</sup>, Nicole Oakman<sup>1</sup>, Lianna Valdes<sup>1</sup>, Betul Bakkaloglu, MD<sup>1</sup>, Niamh Doyle, Ph.D.<sup>2</sup>, Carolyn M. Yrigollen<sup>3</sup>, Thomas M. Morgan, M.D.<sup>4</sup>, and Elena L. Grigorenko, Ph.D.<sup>1,5,6,\*</sup>

<sup>1</sup>Yale University, USA

<sup>2</sup>Syracuse City School District, USA

<sup>3</sup>UC Davis, USA

<sup>4</sup>Vanderbilt University, USA

<sup>5</sup>Columbia University, USA

<sup>6</sup>Moscow State University, Russia

### Abstract

We report the clinical and cytogenetic findings on a male child with developmental language disorder, no physical abnormalities, and a balanced t(10;15)(q24.1;q21.1) translocation. As the child's parents are unavailable for investigations, it is unclear whether the translocation is inherited or *de novo*. Fluorescence in situ hybridization (FISH) analyses were carried out using specific RP11-BAC clones mapping near 15q21.1 and 10q24.1 to refine the location of the breakpoints. The breakpoint on 15q21.1 interrupts the *SEMA6D* gene and the breakpoint on 10q24.1 is located between the *ENTPD1* and *CCNJ* genes. The *SEMA6D* gene was further investigated in samples of individuals with developmental language disorders and controls; this investigation offered further evidence of the involvement of *SEMA6D* with developmental language disorders.

### Keywords

Language disorder; chromosomal aberrations; *SEMA6D*; FISH; *ENTPD1*; *CCNJ*

## 1. Introduction

Language disorders and delays are quite common in pediatric patients, with up to 17% of toddlers and 7.4% of [1,2] kindergarten-age children characterized as having a developmental language disorder (DLD), i.e., systematic deviation in the acquisition of speech and language [2]. DLD appears to be more common among males (8%) than females (6%); the reported estimates vary slightly across different racial/cultural backgrounds [2].

© 2011 Elsevier Masson SAS. All rights reserved.

\*Corresponding Author: Child Study Center, Yale University, 230 South Frontage Road, New Haven, CT 06519, Elena.Grigorenko@Yale.Edu, Phone (203) 737-2316 Fax (203) 785-3002.

**Publisher's Disclaimer:** This is a PDF file of an unedited manuscript that has been accepted for publication. As a service to our customers we are providing this early version of the manuscript. The manuscript will undergo copyediting, typesetting, and review of the resulting proof before it is published in its final citable form. Please note that during the production process errors may be discovered which could affect the content, and all legal disclaimers that apply to the journal pertain.

The etiology of DLD is unknown, but thought to be complex with a substantial genetic basis [3]. Numerous studies have investigated the genetic bases of DLD, yet the specific mechanism is unclear. What is assumed is that DLD is characterized by multifactorial polygenic transmission in the general population and specific rare mutations (e.g., in the *FOXP2* gene) in selected families. Susceptibility loci and candidate genes, identified cytogenetically and statistically, include 2p22, 16q24, 19q13, *FOXP2*, *CMIP* and *ATP2C2* [3], respectively. Here we describe a balanced translocation 46,XY,t(10;15)(q24.1;q21.1) in a male child with DLD and introduce an additional candidate gene for DLD.

## 2. Material and Methods

### 2.1. Clinical Report

The child, adopted from Russia at the age of nine months, was evaluated twice at Yale University (at 3;0 and 4;1 years of age). Due to the early history of the child, the birth record is limited and, per the adoptive mother's report, the record indicated that the child was born at normal weight (2,970 grams) with hypotrophy I degree, general weakness of the CNS attributed to birth trauma, delays in gross-motor development, and sleep problems. The child also had a history of persistent ear and sinus infections, and had both tonsils and adenoids removed and PE tubes placed in both ears. The first evaluation in the US was carried out when the child was 28 months old, when the adoptive parents became concerned with the child's progress, especially language development. As recorded by the child's pediatrician in the USA, growth measurements were in the lower normal range; no dysmorphology was noted. Following this evaluation, the child was diagnosed with Developmental Delays (Language and Fine Motor Skills), Oral Motor Dysfunction, Sensory Integration Disorder, Post-Institutional Response Syndrome, and Chromosomal Abnormality. A brain MRI investigation did not reveal any noticeable structural abnormalities. Since the first evaluation, the boy has been evaluated multiple times, and, overall, demonstrates steady improvement in functioning. Throughout these evaluations, he has shown below average to average nonverbal intelligence along with severely challenged language development with deficits in a variety of linguistic domains (speech and sound, receptive and expressive language). No social-emotional dysfunction was either reported or observed during his evaluations at Yale University. At 3 years, he was assessed with the *Reynell Developmental Language Scales* (RDLS) and demonstrated a significant delay in both expressive and receptive communication; his language skills were close to untestable. At 4 years, the boy was assessed with the *Comprehensive Assessment of Spoken Language* (CELF) and scored in the 1<sup>st</sup> and 2<sup>nd</sup> percentile across multiple domains of linguistic functioning. Thus, at that time, the boy had virtually no expressive language and little receptive language, whereas nonverbal functioning was at the average level (*Wechsler Preschool and Primary Scale of Intelligence*, WPPSI, PIQ=100).

### 2.2. FISH Mapping

An apparently balanced t(10;15)(q24;q21) translocation was identified in our patient with conventional G-banding on metaphase chromosomes from blood lymphocyte cultures. Subsequently, the chromosomal abnormality was fine-mapped using fluorescent *in situ* hybridization (FISH) as described previously [4]. FISH hybridization was performed in metaphase chromosome preparations from the patient using different bacterial artificial chromosomes (BACs) corresponding to regions predicted to contain both breakpoints. The BACs were identified in the UCSC Genome Browser (NCBI36/hg18) and obtained from the Roswell Park Cancer Institute (RPCI-11) library. To localize the breakpoints of the translocation, we performed a systematic series of FISH analyses using 25 and 27 different BAC clones corresponding to the 15q21 and 10q24 regions, respectively. Overlapping BAC clones RP11-652G4 and RP11-313A9 were found to span the chromosome 15q breakpoint

located on base pairs 45,424,164-45,561,018. The breakpoint on chromosome 10q mapped to base pairs 97,613,089- 97,781,640, and this region contains 3 spanning BAC clones RP11-248J23, RP11-635L4 and RP11-959B15. We constructed a BAC contig map with UCSC databases to show both flanking and spanning BACs at each breakpoint region.

### 2.3. Expression Studies

Real-time RT-PCR was used to quantify the small changes in gene expression. In performing real time RT-PCR, first mRNA was isolated from the Epstein-Barr virus immortalized lymphoblastoid cell line using the RNeasy kit (Qiagen). Then DNase treated mRNA was reverse transcribed into cDNA according to the manufacturer's instructions (Omniscript RT kit). Primers were designed using Primer Express Software (ABI) on the exon-exon junction, and tested for specificity using NCBI's BLAST software. The PCR efficiency of each primer was calculated by plotting the Threshold cycle (Ct) as a function of the Log10 concentration of the template used. All of the primers' PCR efficiencies were uniformly >90% (slope=-3.2 and -3.6 and  $R^2$  99%). All reactions were carried out in triplicate with the ABI Prism 7900 high-throughput sequence detection system using Applied Biosystems' standard thermal cycling parameters. Gene expression was calculated using the  $\Delta\Delta C_t$  method.

### 2.4. Mutation Screening and TaqMan Genotyping

All coding exons and 30bp of the flanking intron-exon boundaries of the *SEMA6D* gene were amplified using a sample of 368 individuals with DLD from Russia. PCR products were screened to detect any missense, nonsense and splice-site *SEMA6D* mutations by Sanger sequencing (Beckman Genomics, Beverly, MA). Similarly, using Sanger sequencing, we screened 360 control individuals of diverse EuroAsian ethnic backgrounds for variants in *SEMA6D*. All of the primers were designed using Primer3 (v.0.4.0) software. The sequence results were analyzed using Sequencher 4.9 software. Any missense variants found were evaluated for conservation across diverse species with a ClustalW alignment. Also, these variants were examined using amino acid analysis algorithms PolyPhen-2 (Polymorphism Phenotyping v2) and Sorting Tolerant From Intolerant (SIFT) to identify the amino acid substitutions affecting protein function. The missense mutations found in cases were further investigated using Custom TaqMan SNP Genotyping Assays (ABI) in a sample of 1230 unrelated individuals from The National Institute of Neurological Disorders and Stroke (NINDS)—a neurologically normal control set.

### 2.5. Copy Number Variants (CNVs)

We screened for other small chromosomal abnormalities in our patient using The Illumina Human CNV370-Duo chips. Also, CNVs were evaluated for the genes identified on breakpoints by investigating a sample of 284 individuals with DLD from Russia using The Illumina Human CNV370-Duo chips (genotypes >370,000 loci with 5.0kb median marker spacing). Each individual's scanned data were visualized using the BeadStudio software package version 3.2.23, with the Human Genome Build 18 as reference. CNVs were predicted using PennCNV (PN), a hidden Markov model (HMM) based approach [5], QuantiSNP (QS), Objective Bayes Hidden-Markov Model (OB-HMM) [6] and GNOSIS (GN), based on a distribution function algorithm designed in Dr. State's laboratory (<http://www.yale.edu/statelab>). Results from these three algorithms were merged using an in-house Perl script, CNVision (<http://www.yale.edu/statelab>). Based on a blind analysis of detection accuracy for 115 CNVs, only those predicted by PN and QS with or without agreement from GN were pursued further.

### 3. Results

We found a balanced translocation in a male child with DLD using conventional G-banding. This translocation was the only chromosomal abnormality detectable by this technique. Subsequent CNV analysis on our patient using The Illumina Human CNV370-Duo chips did not detect any other rare loss or gain. Since the patient was adopted, we were unable to locate his biological parents. The 15q21.1 breakpoint maps to the overlap of the BAC clones RP11-652G4 and RP11-313A9 and in between the flanking BACs RP11-408J6 and RP11-142E8. The break in chromosome 15 disrupted the *SEMA6D* (Semaphorin 6D) gene isoform 1. Also this breakpoint was approximately 372 kb away from the other isoforms of *SEMA6D* gene (Figure A, B). The 10q24.1 breakpoint maps to base pairs 97,613,089-97,781,640 within the shared region of BACs RP11-248J23, RP11-635L4 and RP11-959B15. The BAC clone RP11-429G19 is proximal to the breakpoint on 10q24.1 and BAC RP11-690P14 is distal. This indicates that the gene *ENTPD1* (ectonucleoside triphosphate diphosphohydrolase) is ~42 kb centromeric to the chromosomal break and *CC2D2B* (Homo sapiens cDNA FLJ41429 fis; coiled-coil and C2 domain containing 2B) is ~80 kb telomeric (Figure A, C). A real-time RT-PCR technique showed no predictable *SEMA6D* expression using the peripheral blood mRNA of controls (data not shown); correspondingly, its expression in our patient's lymphocytes was not investigated.

A sample of 368 Russian patients with DLD was screened for mutations in *SEMA6D* using Sanger sequencing. We found two missense variants; I240V and L224F on the SEMA domain of the gene in patient 1 and patient 2 of 368 Russian patients, respectively (Table). These variants were evaluated for conservation across diverse species with a ClustalW2 program alignment; both are highly conserved. SIFT and PolyPhen algorithms identified these missense mutations as affecting the protein function. The segregation analysis showed that the I240V variant was *de novo*, and also found that in the affected sister of patient 1, the absence of the I240V variant in lymphocyte DNA from the parents is consistent with germline mosaicism [7]. The L224F variant was present in patient 2 only, and it is a *de novo* event. These variants were not found in 1230 control samples. A further investigation of an ethnically matched subset (n=360) of controls using Sanger sequencing resulted in the identification of two missense mutations not placed on any protein domain of *SEMA6D*. A review of The Database of Genomic Variants (<http://projects.tcag.ca/variation/>) for the CNVs of *SEMA6D* and other breakpoint genes showed that there are 2 intronic duplications and 3 intronic losses in *SEMA6D*, an exonic loss in *ENTPD1*, and an intronic loss in *CCNJ* in individuals of Asian ancestry. Yet, our CNV analyses of the additional 284 individuals with DLD for the *SEMA6D*, *CCNJ* and *ENTPD1* loci did not detect any losses or gains.

### 4. Discussion

Chromosomal rearrangements are important etiological factors for many disorders, including DLD. Of the 3 genes disrupted by 46,XY,t(10;15)(q24.1;q21.1) in our patient, we focused on *SEMA6D* because it has a plausible role in DLD. The semaphorin gene family is known to provide axon guidance cues during the development of the nervous system [8]. *SEMA6D* is highly expressed in areas of the lateral ventricle, the striatum, the wall of the midbrain, the pons/midbrain junction, and the choroid plexus of murine embryos (E13) [9]. All semaphorins contain a semaphorin (sema) domain and a PSI domain (found in plexins, semaphorins, and integrins) in the extracellular portion [10]. Analysis of plexinA1 mutant mice reveals that the sema6D transmembrane protein acts as a ligand for plexinA1, and sema6D-plexinA1 signaling in sensory neuron development controls proprioceptive axon shaft position [11]. The semaphorin gene family has been reported to be linked to a number of developmental disorders. Specifically, *SEMA5A* has been associated with autism [12,13], *SEMA3A* with schizophrenia [14], and *SEMAF* with mental retardation in Cri-du-chat

[15]. Moreover, *SEMA3B* is thought to be a potential transcriptional target for *FOXP2* [16], a gene that has been identified in a complex genomic disorder characterized by, among others, a language impairment [17]. Finally, the 15q21 region harboring *SEMA6D* has been implicated in a variety of developmental disorders, including dyslexia, stuttering, and autism [3].

Although investigated to a lesser extent here, *ENTPDI* and *CCNJ* are of interest to studies of DLD as well. *ENTPDI*, or ecto-nucleoside triphosphate diphosphohydrolase, belongs to the CD39 family, which comprises integral membrane proteins with large extracellular domains. By regulating the hydrolysis of important signaling nucleotides (e.g. ATP to AMP), these proteins help control several important brain activities, including interactions between neurons and glial cells, hemostatic and inflammatory responses, and the regulation of blood flow [18]. *CCNJ* belongs to the cyclin family of proteins, which help regulate the cell cycle by controlling the activity of cyclin-dependent kinases [19]. Therefore, *CCNJ* may be an important regulator of neural development during embryogenesis.

In summary, here we report findings on a patient with DLD (profound expressive language delay, severe receptive level delay, and average nonverbal ability) and balanced translocation on chromosomes 15q21.1 (interrupting the *SEMA6D* gene) and 10q24.1 (located between the *ENTPDI* and *CCNJ* genes). In addition, we provide further evidence of the potential involvement of variations in *SEMA6D* with DLD by studying two independent samples of individuals with DLD, and gain further evidence of the relevance of the variation in this gene to the manifestation of DLD. Yet, additional research is necessary to draw more specific genotype–phenotype correlations.

## Acknowledgments

The preparation of this article was supported by funds from the Foundation for Child Development (PI Grigorenko) and the US National Institutes of Health, NIH (awards DC007665, PI Grigorenko, and HD052120, PI Wagner). Grantees undertaking such projects are encouraged to freely express their professional judgment. This article, therefore, does not necessarily represent the position or policies of the NIH and no official endorsement should be inferred. We are thankful to Drs. Lesley Hart and Tina Newman, Ms. Donna Macomber, and graduate students in clinical psychology at Yale University for their contributions to the clinical evaluations of this patient. We are also thankful to Ms. Mei Tan for her editorial assistance. Last, and foremost, we are grateful to the patient's family.

## References

1. Rescorla L. The Language Development Survey: a screening tool for delayed language in toddlers. *J Speech Hear Disord.* 1989; 54:587–599. [PubMed: 2811339]
2. Tomblin JB, Records NL, Buckwalter P, Zhang X, Smith E, O'Brien M. Prevalence of specific language impairment in kindergarten children. *J Speech Lang Hear Res.* 1997; 40:1245–1260. [PubMed: 9430746]
3. Grigorenko EL. Speaking genes or genes for speaking? Deciphering the genetics of speech and language. *J Child Psychol Psychiatry.* 2009; 50:116–125. [PubMed: 19220595]
4. Lichter P, Ledbetter SA, Ledbetter DH, Ward DC. Fluorescence in situ hybridization with Alu and L1 polymerase chain reaction probes for rapid characterization of human chromosomes in hybrid cell lines. *Proc Natl Acad Sci U S A.* 1990; 87:6634–6638. [PubMed: 2395866]
5. Wang K, Li M, Hadley D, Liu R, Glessner J, Grant SF, Hakonarson H, Bucan M. PennCNV: an integrated hidden Markov model designed for high-resolution copy number variation detection in whole-genome SNP genotyping data. *Genome Res.* 2007; 17:1665–1674. [PubMed: 17921354]
6. Colella S, Yau C, Taylor JM, Mirza G, Butler H, Clouston P, Bassett AS, Seller A, Holmes CC, Ragoussis J. QuantiSNP: an Objective Bayes Hidden-Markov Model to detect and accurately map copy number variation using SNP genotyping data. *Nucleic Acids Res.* 2007; 35:2013–2025. [PubMed: 17341461]
7. Zlotogora J. Germ line mosaicism. *Hum Genet.* 1998; 102:381–386. [PubMed: 9600231]

8. Toyofuku T, Yoshida J, Sugimoto T, Yamamoto M, Makino N, Takamatsu H, Takegahara N, Suto F, Hori M, Fujisawa H, Kumanogoh A, Kikutani H. Repulsive and attractive semaphorins cooperate to direct the navigation of cardiac neural crest cells. *Dev Biol.* 2008; 321:251–262. [PubMed: 18625214]
9. Qu X, Wei H, Zhai Y, Que H, Chen Q, Tang F, Wu Y, Xing G, Zhu Y, Liu S, Fan M, He F. Identification, characterization, and functional study of the two novel human members of the semaphorin gene family. *J Biol Chem.* 2002; 277:35574–35585. [PubMed: 12110693]
10. Bork P, Doerks T, Springer TA, Snel B. Domains in plexins: links to integrins and transcription factors. *Trends Biochem Sci.* 1999; 24:261–263. [PubMed: 10390613]
11. Yoshida Y, Han B, Mendelsohn M, Jessell TM. PlexinA1 signaling directs the segregation of proprioceptive sensory axons in the developing spinal cord. *Neuron.* 2006; 52:775–788. [PubMed: 17145500]
12. Melin M, Carlsson B, Anckarsater H, Rastam M, Betancur C, Isaksson A, Gillberg C, Dahl N. Constitutional downregulation of SEMA5A expression in autism. *Neuropsychobiology.* 2006; 54:64–69. [PubMed: 17028446]
13. Weiss LA, Arking DE, Daly MJ, Chakravarti A. A genome-wide linkage and association scan reveals novel loci for autism. *Nature.* 2009; 461:802–808. [PubMed: 19812673]
14. Eastwood SL, Law AJ, Everall IP, Harrison PJ. The axonal chemorepellant semaphorin 3A is increased in the cerebellum in schizophrenia and may contribute to its synaptic pathology. *Mol Psychiatry.* 2003; 8:148–155. [PubMed: 12610647]
15. Simmons AD, Puschel AW, McPherson JD, Overhauser J, Lovett M. Molecular cloning and mapping of human semaphorin F from the Cri-du-chat candidate interval. *Biochem Biophys Res Commun.* 1998; 242:685–691. [PubMed: 9464278]
16. Spiteri E, Konopka G, Coppola G, Bomar J, Oldham M, Ou J, Vernes SC, Fisher SE, Ren B, Geschwind DH. Identification of the transcriptional targets of FOXP2, a gene linked to speech and language, in developing human brain. *Am J Hum Genet.* 2007; 81:1144–1157. [PubMed: 17999357]
17. Fisher SE, Vargha-Khadem F, Watkins KE, Monaco AP, Pembrey ME. Localisation of a gene implicated in a severe speech and language disorder. *Nature Genetics.* 1998; 18:168–170. [PubMed: 9462748]
18. Braun N, Sevigny J, Robson SC, Enyoji K, Guckelberger O, Hammer K, Di Virgilio F, Zimmermann H. Assignment of ecto-nucleoside triphosphate diphosphohydrolase-1/cd39 expression to microglia and vasculature of the brain. *Eur J Neurosci.* 2000; 12:4357–4366. [PubMed: 11122346]
19. Kolonin MG, Finley RL Jr. A role for cyclin J in the rapid nuclear division cycles of early *Drosophila* embryogenesis. *Dev Biol.* 2000; 227:661–672. [PubMed: 11071782]



- We report a male child with a balanced t(10;15)(q24.1;q21.1) translocation.
- Breakpoints on chromosomes 15q21.1 interrupt the *SEMA6D* gene; the other breakpoint 10q24.1 disrupts the *ENTPDI* and *CCNJ* genes.
- We argue that language functioning is a main target of this genomic lesion.

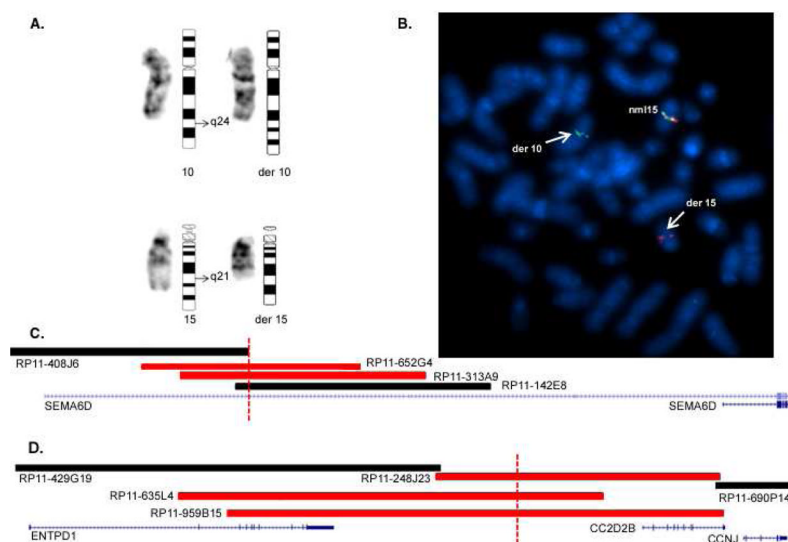


### Figure.

(A and B) Ideogram and partial karyotype of the patient showing derivative chromosomes resulting from a  $t(10;15)(q24.1;q21.1)$  balanced translocation. Chromosome breakpoints are indicated by arrows. Metaphase spreads of the patient with DAPI-banding and with FISH probes for the two flanking BAC clones on chromosome 15. RP11-408J6 are labeled with Cy3 (red signal), and RP11-142E8 is labeled with FITC (green signal). Both red and green signals are present on the normal 15 (nml,15) chromosome as expected. Arrows indicate the derivative chromosomes having hybridization signals for only 1 probe. A Cy3 signal is detected on der (15) indicating that the BAC is located proximal to the break, and a FITC signal is present on der (10) showing the probe localized distal to the break. (C) Diagram of the interval flanking the spanning RP11-652G4, and RP11-313A9 BACs at 15q21.1. The SEMA6D isoform 1 maps approximately 372 kb telomeric to the break. (D) Diagram of the interval flanking the spanning RP11-248J23, RP11-635L4 and RP11-959B15 clones at 10q24.1. The gene ENTPD1 maps approximately 42 kb and CC2D2B gene maps ~80 kb to the break. Dashed lines indicate the approximate location of the break. (Horizontal black BAC clones are flanking and red BAC clones are spanning).



**Table**  
*SEMA6D* gene missense mutations found in patients with language disorder and control samples

Exon	Nucleotide Variation	AminoAcid Substitution	Segregation Analysis	Allele Frequency *	Conservation	Domain
9	A/G	I240V	2 (patient1 and his affected sibling	0.0013	conserved	SEMA
9	T/C	L224F	1(patient2)	0.0013	conserved	SEMA
Controls						
19	C/T	P765L	1	0.0013	conserved	N/A
19	A/T	E926V	1	0.0013	conserved	N/A

\* The allele frequencies for probands' and controls' mutations were estimated to be 1/736 and 1/720, respectively.